ISSN 0915-633X

NATIONAL INSTITUTE FOR FUSION SCIENCE

Computer Has Solved A Historical Puzzle: Generation of Earth's Dipole Field

A. Kageyama, T. Sato and The Complexity Simulation Group

(Received - May 17, 1995)

NIFS-359 June 1995

RESEARCH REPORT
NIFS Series

NAGOYA, JAPAN

Computer Has Solved A Historical Puzzle: Generation of Earth's Dipole Field

Akira Kageyama, Tetsuya Sato and The Complexity Simulation Group†

Theory and Computer Simulation Center,
National Institute for Fusion Science, Nagoya 464-01, Japan

Computer simulation of a magnetohydrodynamic dynamo is performed. It is found that strong dipole field is self-consistently and preferentially excited by thermal convection of an electrically conducting fluid in a rapidly rotating spherical shell. Thus, the long standing puzzle of the origin of the earth's dipole field is finally resolved. It is also found that radial components of the generated magnetic field are accumulated, with equal intensity and polarity, in all cyclonic convection columns near the outer spherical boundary. This is the reason that the dipole moment becomes dominant over other moments. Therefore, we can conclude that the preferential excitation of the dipole field is a natural consequence of well-organized convection columns.

keywords dynamo, geodynamo, MHD dynamo

†R. Horiuchi, K. Watanabe, T. Hayashi, Y. Todo, T. H. Watanabe, H. Takamaru and S. V. Bazdenkov

In 1600, dipole dominance in the earth's magnetic field was pointed out by Gilbert[1]. Two hundred years later, in 1839, Gauss attempted to make a diagnosis of the global distribution of the geomagnetic field by placing the magnetometer in many places to confirm its dipole dominance[1]. Toward the middle of twentieth century, a real scientific challenge started revealing how the geomagnetic field is generated in the interior of a planet like the earth, namely, the dynamo mechanism[2–8]. Many analytical attempts have been made to elucidate the mechanism, but no quantitative result is obtained. The invention of supercomputer has shed a light on revealing it. In fact, in these ten years several attempts[9–12] to demonstrate generation of magnetic fields by computer simulations have been done with partial success in generating the magnetic field. But they are all far from complete. Very recently, Kageyama and Sato[13] have succeeded in generating the magnetic field whose energy becomes much larger than the convection (Benard cell) energy. The work, however, has not been able to demonstrate the preferential excitation of the dipole component. We have made elaborate efforts to resolve the problem, and at last discovered that the dipole field is self-consistently and preferentially excited from the convection columns generated by the convection instability originating from a heat source in the central core of the earth's interior such as radioactivity. Thus, the long standing puzzle of generating the earth's dipole field, which is believed to have almost the same age as the earth, is finally resolved.

Our simulation model is a rotating sphere with a constant angular velocity (see Fig.1a). The sphere consists of an inner spherical core that has a heat source to keep its surface ($r = r_i$) at a high temperature (T_h), an outer heat absorbing spherical boundary surface ($r = r_o$) which is kept at a low temperature (T_ℓ), and an intermediate conductive fluid medium sandwiched by the two spherical boundaries ($r = r_i$ and r_o) with different temperatures (T_h and T_ℓ). The conductive medium is represented by a set of compressible, resistive magnetohydrodynamic equations with gravity force. The medium is implemented on a spherical coordinate (r, ϑ, φ) grid point system. We impose a symmetry condition at the equatorial plane ($\vartheta = 90°$), namely, $v_\vartheta = B_r = B_\varphi = 0$ and vanishing of the latitudinal derivative of the other components, so that we can solve only one (northern) hemisphere. The grid numbers $(N_r, N_\vartheta, N_\varphi)$ are taken to be $(50, 20, 64)$ and $(80, 40, 128)$ to confirm that both simulations yield the same results, namely, that the numerical resolution is sound. The boundary condition is such that $\mathbf{v} = E_r = \frac{\partial E_\vartheta}{\partial r} = \frac{\partial E_\varphi}{\partial r} = 0$ at $r = r_i$ and r_o. The parameters used in this simulation are as follows: $r_i = 0.3$, $r_o = 1.0$, $R = 1 \times 10^4$, $Rm = 3.33 \times 10^2$, $T = 5.88 \times 10^6$, $Pr = 1$, $Pr_m = 9.43$, where R, Rm, T, Pr, Pr_m are Raleigh number, Magnetic Reynolds number, Taylor number, Prandtl number, Magnetic Prandtl number, respectively. Some of these parameters may not well fit those of the real earth's environment partly because of the lack of sufficient observational data and partly because of the limit of the present-day supercomputer. But we believe that the present model does include the essential physics of the geodynamo.

A thermal convection instability, with no magnetic field, grows when a weak random noise is superimposed upon the initial temperature profile. Well-organized anti-cyclonic and cyclonic columnar cells, or, anti-cyclonic and cyclonic convection columns, whose axes are beautifully aligned along the rotation axis, are formed in an alternating fashion so as to encircle the rotation axis[14,15] (see Fig.1b).

Temporal developments of the total convection (kinetic) energy and the total magnetic energy are shown in Fig. 2a. The convection energy saturates at a relatively early time, i.e., $t = 150$ in the time unit of r_o/c_s (c_s: sound speed).

After the convection columns have reached to a steady state ($t = 256$), we superimpose a seed of random magnetic field components upon it. Initially the magnetic field experiences damping so as to self-adjust itself to a linear eigenfunction ($t \leq 1500$). Then it starts growing exponentially with a linear growth rate. During this linear growth phase of magnetic energy, $1500 < t < 4500$, the kinetic energy suffers no apparent influence. More surprisingly, the magnetic energy grows beyond the kinetic energy and saturates at an energy level substantially larger than the kinetic energy.

Since the radial component of the magnetic field B_r appearing on the outer boundary ($r = r_o$) yields the potential field component above the surface, we expand $B_r(r_o)$ by means of spherical harmonics Y_ℓ^m. Fig. 2b shows temporal developments of dominant three moments. One can discover a very important and attractive fact that the dipole moment ($\ell = 1, m = 0$)

is the most dominant mode among others.

More directly and intuitively, we illustrate in Fig. 3 color pictures of how the dipole field is spontaneously and preferentially generated. Azimuthally-averaged poloidal magnetic component is shown by thick solid lines (yellow) and toroidal component is shown by color contours: Red (blue) denotes eastward (westward) toroidal field.

Careful examination indicates that radial components of the magnetic field are accumulated, with equal intensity and polarity, in all cyclonic columns near the outer boundary (r_o). From this fact we can conclude that the preferential excitation of the dipole field is a natural consequence arising from well organized cyclonic and anti-cyclonic convection columns[13,15] (Fig.1b). Incidentally, Gubbins and Bloxham[16] have deduced from the earth's surface data that geomagnetic fluxes at the core-mantle boundary are localized in discrete regions. They also have deduced that the positions of the concentrated flux are consistent with convection columns parallel to the rotation axis and tangential to the inner core. These features are in good agreement with our findings.

Computer has thus finally revealed a historical puzzle of mankind, namely, the origin of the earth's dipole field after 160 years passage since Gauss's finding of the dipole dominance in the earth's magnetic field and sixty years theoretical struggles by many researchers since Cowling.

1. See, for example, Rikitake, T., *Electromagnetism and the Earth's Interior*, p.9, Elsevier Publishing Company, Amsterdam, 1966

2. Cowling, T.G., *Monthly Notices Roy. Astron. Soc.*, **94**, 39-48, 1934; *Magnetohydrodynamics*, Interscience, New York, 1957

3. Elsasser, W.M., *Phys. Rev.*, **69**, 106-116, 1946

4. Bullard, E.C. and Gellman, H., *Phil. Trans. Roy. Soc.*, **A247**, 213-278, 1954

5. Braginskii, S.I., *Sov. Phys. JETP*, **20**, 726-735, 1964; ibid. **20**, 1462-1471, 1964

6. Jacobs, J.A., *The earth's core*, second edition, p.192, Academic Press, London, 1987

7. Moffatt, H.K., *Magnetic Field Generation in Electrically Conducting Fluids*, Cambridge University Press, London, 1978

8. Krause, F. and Radler, K.H., *Mean Field Magnetohydrodynamics and Dynamo Theory*, Pergamon Press, Oxford, 1980

9. Gilman, P.A. and Miller, J., *Astrophys. J. Suppl.*, **46**, 211-238, 1981

10. Gilman, P.A., *Astrophys. J. Suppl.*, **53**, 243-268, 1983

11. Glatzmaier, G.A., *J. Comp. Phys.*, **55**, 461-484, 1984

12. Glatzmaier, G.A., *Astrophys. J.*, **291**, 300-307, 1985

13. Kageyama, A and Sato, T., *Phys. Plasmas*, in press, 1995

14. Busse, F.H., *J. Fluid Mech.*, **44**, 441-460, 1970

15. Kageyama, A, Sato, T. and Watanabe, K., *Phys. Fluids B*, **5**, 2793–2805, 1993

16. Gubbins, D and Bloxham, J, *Nature*, **325**,509-511, 1987

This work is supported by Grant-in-Aid from the Ministry of Education, Science and Culture in Japan.

Figure Captions

Fig.1a) Simulation model for studying the geodynamo. The interior of the model is exposed by cutting a piece of the sphere. The green part represents the equatorial plane and the yellow does two meridional planes. The meshes indicated in these planes illustrate how the system is implemented on a grid point system. In the actual simulation the system consists of $(50, 20, 64)$ or $(80, 40, 128)$. The number of the grids shown here does not represent the actual one but is reduced for brevity. An electrically conducting fluid is sandwiched by two concentric spheres with different temperatures; hot (red) and cold (violet). The system is rotating with a constant angular velocity as shown by arrows.

b) Columnar convection cells (convection columns) obtained by simulation with no magnetic field. An important, attractive finding is that the constant axial vorticity contours exhibit a well-organized structure, which forms columnar shapes aligned along the rotation axis. The cyclonic columns (green) and anti-cyclonic columns (yellow) appear in an alternate way to encircle the rotation axis.

Fig.2a) Temporal developments of the kinetic (convection) energy and magnetic energy. When the convection pattern has reached to a steady state ($t = 150$), a tiny seed of random magnetic perturbation is imposed. After the initial adjustment (damping of the magnetic energy), the magnetic perturbation starts growing with a linear exponential growth rate ($t \sim 1000$). At about $t \sim 5100$, the magnetic energy grows beyond the level of the kinetic energy and saturates at a level two times larger than the kinetic energy.

b) Temporal developments of the most dominant three moments of generated magnetic field. Radial component of the magnetic field is expanded by means of spherical harmonics Y_ℓ^m. From this result one can find that the dipole moment ($\ell = 1, m = 0$) is preferentially excited and remains the most dominant component even at a saturated stage. The present simulation is the first demonstration of preferential excitation of the dipole field in a rotating sphere with a heat source at the core part.

Fig.3 A direct demonstration providing the generation of a dipole-like magnetic field in a rotating sphere with a heat source in its interior. The three panels show three time sequential color plots of the azimuthally-averaged meridional (poloidal) component of the generated magnetic field in a meridian plane (yellow). The number of lines represents the intensity of the field. The bright disc-like region represents the simulation region where the innermost part is the hot temperature boundary and the outermost is the low temperature boundary. The reddish part is the color contour of the averaged eastward toroidal field and the bluish is that of the westward one. One can confirm from these color plots that the dipole-dominant field originates from the pair of the eastward (northern hemisphere) and westward (southern hemisphere) components of the toroidal field.

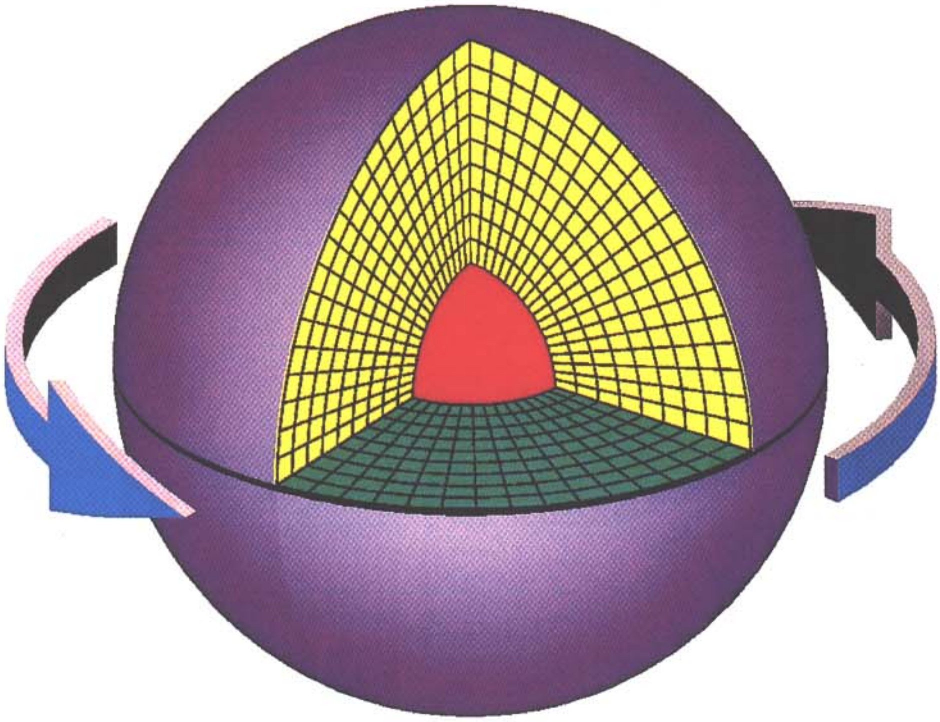

Fig.1a

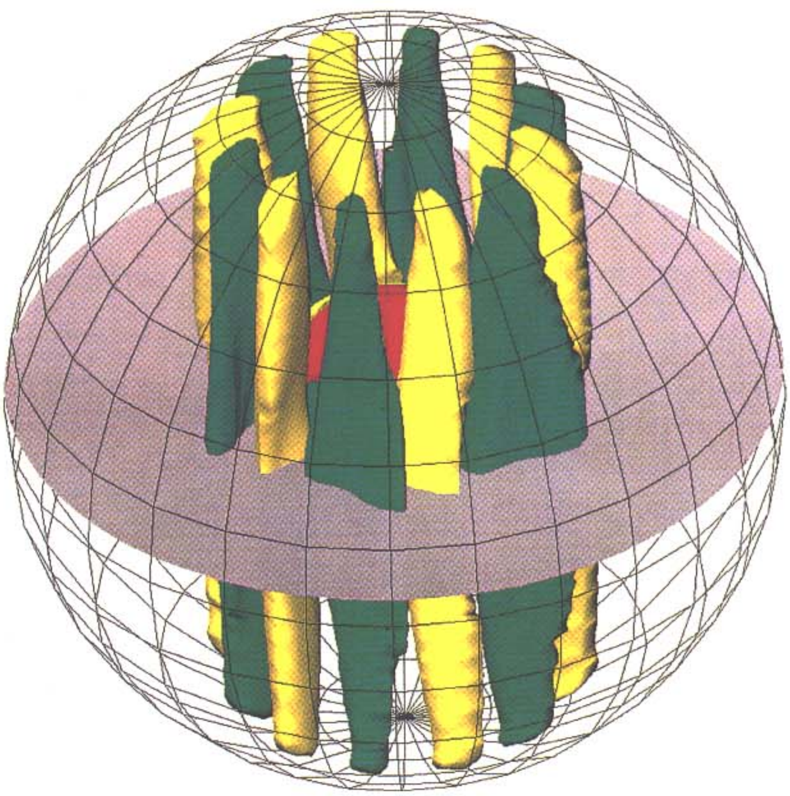

Fig.1b

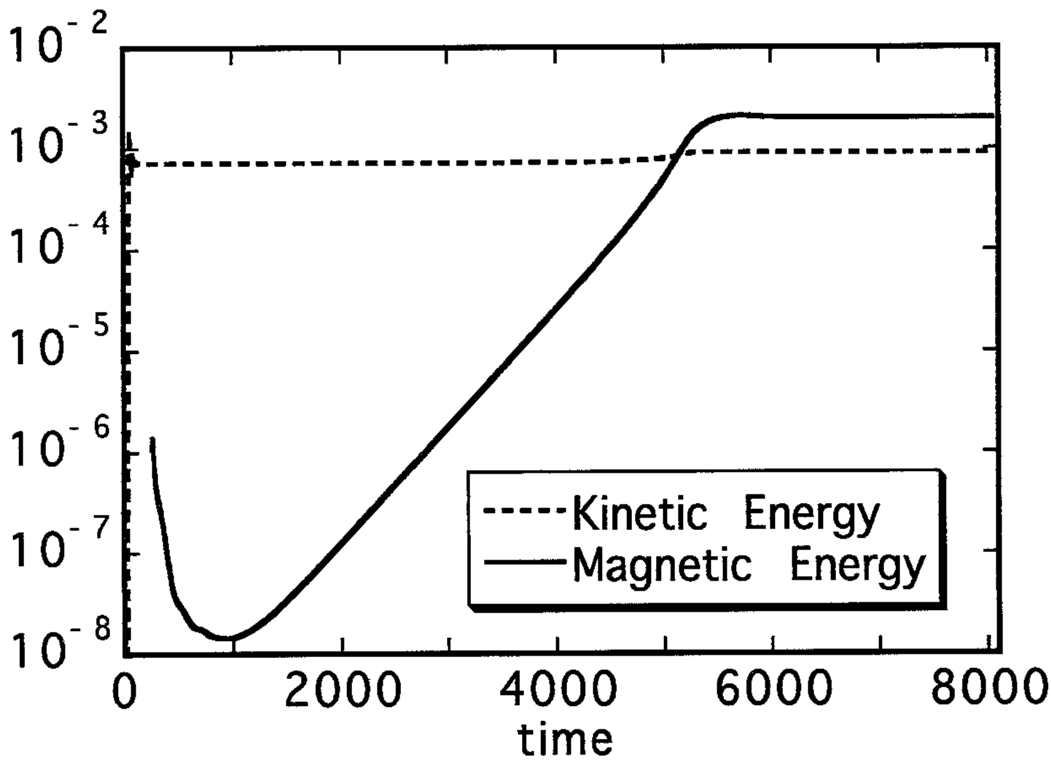
10^{-2}
10^{-3}
10^{-4}
10^{-5}
10^{-6}
10^{-7}
10^{-8}
0
2000
4000
6000
8000
time
Kinetic Energy
Magnetic Energy

Fig.2a

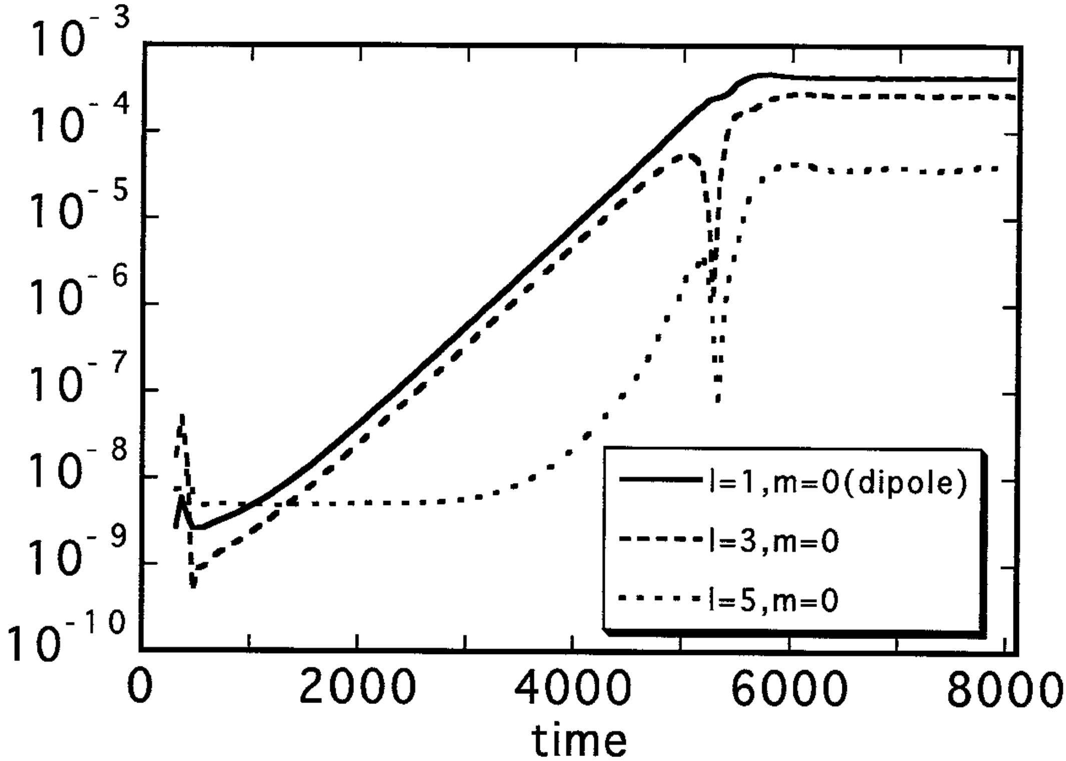

10^{-3}
10^{-4}
10^{-5}
10^{-6}
10^{-7}
10^{-8}
10^{-9}
10^{-10}
0
2000
4000
6000
8000
time
l=1,m=0(dipole)
l=3,m=0
l=5,m=0

Fig.2b

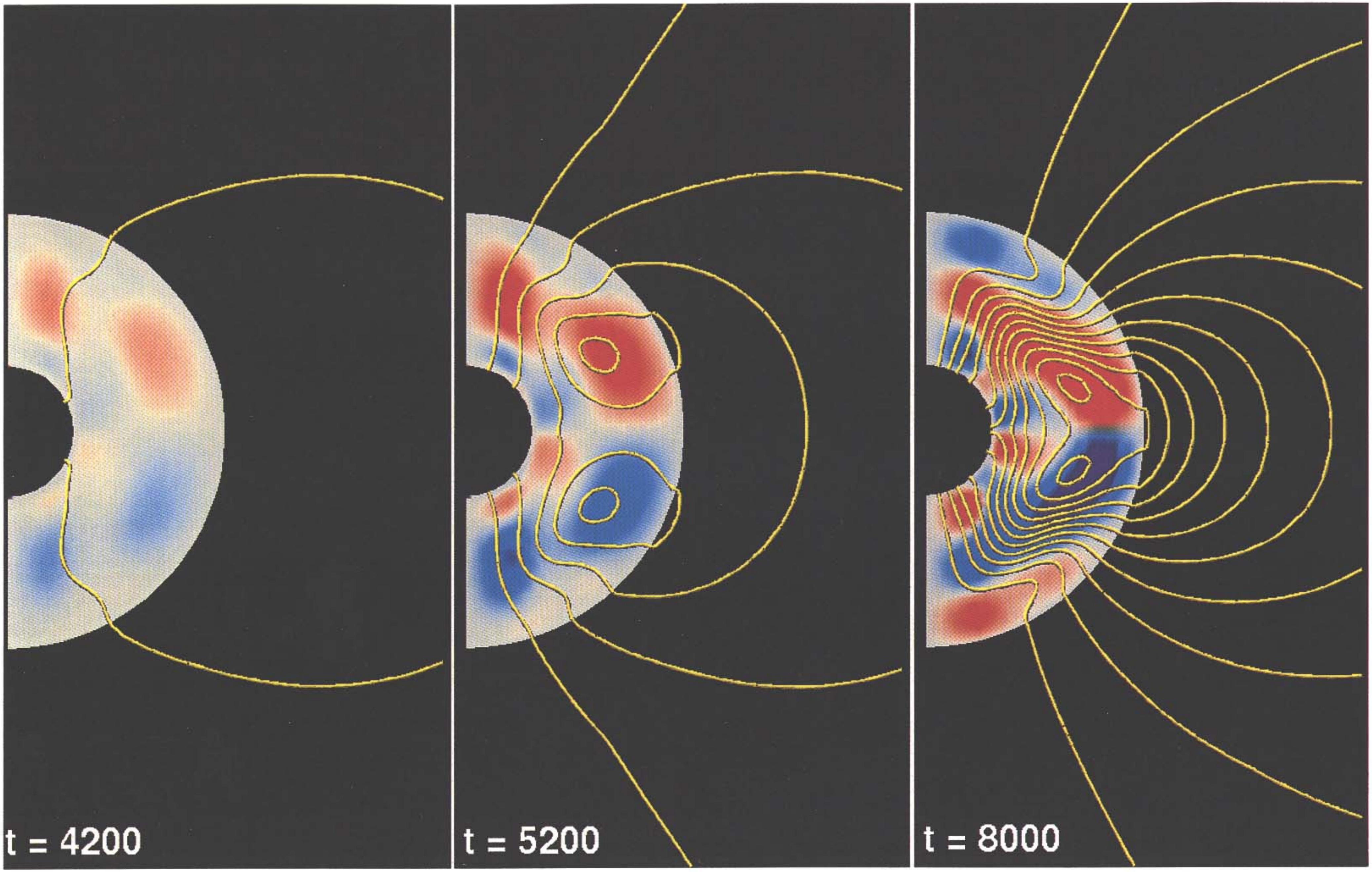

Fig.3

Recent Issues of NIFS Series

NIFS-310 T. Yamagishi and H. Sanuki,
Effect of Anomalous Plasma Transport on Radial Electric Field in Torsatron/Heliotron; Sep. 1994

NIFS-311 K. Watanabe, T. Sato and Y. Nakayama,
Current-profile Flattening and Hot Core Shift due to the Nonlinear Development of Resistive Kink Mode; Oct. 1994

NIFS-312 M. Salimullah, B. Dasgupta, K. Watanabe and T. Sato,
Modification and Damping of Alfvén Waves in a Magnetized Dusty Plasma; Oct. 1994

NIFS-313 K. Ida, Y. Miura, S -I. Itoh, J.V. Hofmann, A. Fukuyama, S. Hidekuma, H. Sanuki, H. Idei, H. Yamada, H. Iguchi, K. Itoh,
Physical Mechanism Determining the Radial Electric Field and its Radial Structure in a Toroidal Plasma; Oct. 1994

NIFS-314 Shao-ping Zhu, R. Horiuchi, T. Sato and The Complexity Simulation Group,
Non-Taylor Magnetohydrodynamic Self-Organization; Oct. 1994

NIFS-315 M. Tanaka,
Collisionless Magnetic Reconnection Associated with Coalescence of Flux Bundles; Nov. 1994

NIFS-316 M. Tanaka,
Macro-EM Particle Simulation Method and A Study of Collisionless Magnetic Reconnection; Nov. 1994

NIFS-317 A. Fujisawa, H. Iguchi, M. Sasao and Y. Hamada,
Second Order Focusing Property of 210° Cylindrical Energy Analyzer; Nov. 1994

NIFS-318 T. Sato and Complexity Simulation Group,
Complexity in Plasma - A Grand View of Self- Organization; Nov. 1994

NIFS-319 Y. Todo, T. Sato, K. Watanabe, T.H. Watanabe and R. Horiuchi,
MHD-Vlasov Simulation of the Toroidal Alfvén Eigenmode; Nov. 1994

NIFS-320 A. Kageyama, T. Sato and The Complexity Simulation Group,
Computer Simulation of a Magnetohydrodynamic Dynamo II: Nov. 1994

NIFS-321 A. Bhattacharjee, T. Hayashi, C.C.Hegna, N. Nakajima and T. Sato,
Theory of Pressure-induced Islands and Self-healing in Three-dimensional Toroidal Magnetohydrodynamic Equilibria; Nov. 1994

NIFS-322 A. Iiyoshi, K. Yamazaki and the LHD Group,
Recent Studies of the Large Helical Device; Nov. 1994

NIFS-323 A. Iiyoshi and K. Yamazaki,
The Next Large Helical Devices; Nov. 1994

NIFS-324 V.D. Pustovitov
Quasisymmetry Equations for Conventional Stellarators; Nov. 1994

NIFS-325 A. Taniike, M. Sasao, Y. Hamada, J. Fujita, M. Wada,
The Energy Broadening Resulting from Electron Stripping Process of a Low Energy Au⁻ Beam; Dec. 1994

NIFS-326 I. Viniar and S. Sudo,
New Pellet Production and Acceleration Technologies for High Speed Pellet Injection System "HIPEL" in Large Helical Device; Dec. 1994

NIFS-327 Y. Hamada, A. Nishizawa, Y. Kawasumi, K. Kawahata, K. Itoh, A. Ejiri, K. Toi, K. Narihara, K. Sato, T. Seki, H. Iguchi, A. Fujisawa, K. Adachi, S. Hidekuma, S. Hirokura, K. Ida, M. Kojima, J. Koong, R. Kumazawa, H. Kuramoto, R. Liang, T. Minami, H. Sakakita, M. Sasao, K.N. Sato, T. Tsuzuki, J. Xu, I. Yamada, T. Watari,
Fast Potential Change in Sawteeth in JIPP T-IIU Tokamak Plasmas; Dec. 1994

NIFS-328 V.D. Pustovitov,
Effect of Satellite Helical Harmonics on the Stellarator Configuration; Dec. 1994

NIFS-329 K. Itoh, S-I. Itoh and A. Fukuyama,
A Model of Sawtooth Based on the Transport Catastrophe; Dec. 1994

NIFS-330 K. Nagasaki, A. Ejiri,
Launching Conditions for Electron Cyclotron Heating in a Sheared Magnetic Field; Jan. 1995

NIFS-331 T.H. Watanabe, Y. Todo, R. Horiuchi, K. Watanabe, T. Sato,
An Advanced Electrostatic Particle Simulation Algorithm for Implicit Time Integration; Jan. 1995

NIFS-332 N. Bekki and T. Karakisawa,
Bifurcations from Periodic Solution in a Simplified Model of Two-dimensional Magnetoconvection; Jan. 1995

NIFS-333 K. Itoh, S.-I. Itoh, M. Yagi, A. Fukuyama,
Theory of Anomalous Transport in Reverse Field Pinch; Jan. 1995

NIFS-334 K. Nagasaki, A. Isayama and A. Ejiri
Application of Grating Polarizer to 106.4GHz ECH System on Heliotron-E; Jan. 1995

NIFS-335 H. Takamaru, T. Sato, R. Horiuchi, K. Watanabe and Complexity Simulation

Group,
A Self-Consistent Open Boundary Model for Particle Simulation in Plasmas; Feb. 1995

NIFS-336 B.B. Kadomtsev,
Quantum Telegragh : is it possible?; Feb. 1995

NIFS-337 B.B.Kadomtsev,
Ball Lightning as Self-Organization Phenomenon; Feb. 1995

NIFS-338 Y. Takeiri, A. Ando, O. Kaneko, Y. Oka, K. Tsumori, R. Akiyama, E. Asano, T. Kawamoto, M. Tanaka and T. Kuroda,
High-Energy Acceleration of an Intense Negative Ion Beam; Feb. 1995

NIFS-339 K. Toi, T. Morisaki, S. Sakakibara, S. Ohdachi, T.Minami, S. Morita, H. Yamada, K. Tanaka, K. Ida, S. Okamura, A. Ejiri, H. Iguchi, K. Nishimura, K. Matsuoka, A. Ando, J. Xu, I. Yamada, K. Narihara, R. Akiyama, H. Idei, S. Kubo, T. Ozaki, C. Takahashi, K. Tsumori,
H-Mode Study in CHS; Feb. 1995

NIFS-340 T. Okada and H. Tazawa,
Filamentation Instability in a Light Ion Beam-plasma System with External Magnetic Field; Feb. 1995

NIFS-341 T. Watanbe, G. Gnudi,
A New Algorithm for Differential-Algebraic Equations Based on HIDM; Feb. 13, 1995

NIFS-342 Y. Nejoh,
New Stationary Solutions of the Nonlinear Drift Wave Equation; Feb. 1995

NIFS-343 A. Ejiri, S. Sakakibara and K. Kawahata,
Signal Based Mixing Analysis for the Magnetohydrodynamic Mode Reconstruction from Homodyne Microwave Reflectometry; Mar.. 1995

NIFS-344 B.B.Kadomtsev, K. Itoh, S.-I. Itoh
Fast Change in Core Transport after L-H Transition; Mar. 1995

NIFS-345 W.X. Wang, M. Okamoto, N. Nakajima and S. Murakami,
An Accurate Nonlinear Monte Carlo Collision Operator; Mar. 1995

NIFS-346 S. Sasaki, S. Takamura, S. Masuzaki, S. Watanabe, T. Kato, K. Kadota,
Helium I Line Intensity Ratios in a Plasma for the Diagnostics of Fusion Edge Plasmas; Mar. 1995

NIFS-347 M. Osakabe,
Measurement of Neutron Energy on D-T Fusion Plasma Experiments; Apr. 1995

NIFS-348 M. Sita Janaki, M.R. Gupta and Brahmananda Dasgupta,
Adiabatic Electron Acceleration in a Cnoidal Wave; Apr. 1995

NIFS-349 J. Xu, K. Ida and J. Fujita,
A Note for Pitch Angle Measurement of Magnetic Field in a Toroidal Plasma Using Motional Stark Effect; Apr. 1995

NIFS-350 J. Uramoto,
Characteristics for Metal Plate Penetration of a Low Energy Negative Muonlike or Pionlike Particle Beam: Apr. 1995

NIFS-351 J. Uramoto,
An Estimation of Life Time for A Low Energy Negative Pionlike Particle Beam: Apr. 1995

NIFS-352 A. Taniike,
Energy Loss Mechanism of a Gold Ion Beam on a Tandem Acceleration System: May 1995

NIFS-353 A. Nishizawa, Y. Hamada, Y. Kawasumi and H. Iguchi,
Increase of Lifetime of Thallium Zeolite Ion Source for Single-Ended Accelerator: May 1995

NIFS-354 S. Murakami, N. Nakajima, S. Okamura and M. Okamoto,
Orbital Aspects of Reachable β Value in NBI Heated Heliotron/Torsatrons; May 1995

NIFS-355 H. Sugama and W. Horton,
Neoclassical and Anomalous Transport in Axisymmetric Toroidal Plasmas with Electrostatic Turbulence; May 1995

NIFS-356 N. Ohyabu
A New Boundary Control Scheme for Simultaneous Achievement of H-mode and Radiative Cooling (SHC Boundary); May 1995

NIFS-357 Y. Hamada, K.N. Sato, H. Sakakita, A. Nishizawa, Y. Kawasumi, R. Liang, K. Kawahata, A. Ejiri, K. Toi, K. Narihara, K. Sato, T. Seki, H. Iguchi, A. Fujisawa, K. Adachi, S. Hidekuma, S. Hirokura, K. Ida, M. Kojima, J. Koong, R. Kumazawa, H. Kuramoto, T. Minami,. M. Sasao, T. Tsuzuki, J.Xu, I. Yamada, and T. Watari,
Large Potential Change Induced by Pellet Injection in JIPP T-IIU Tokamak Plasmas; May 1995

NIFS-358 M. Ida and T. Yabe,
Implicit CIP (Cubic-Interpolated Propagation) Method in One Dimension; May 1995